FA

(19) Japan

(12) Official Gazette for Unexamined Patents (A)

(11) Kokai No. 63-305082
(Published unexamined patent application)

(43) Kokai publication date: December 13, 1988

(22) Application date: June 5, 1987

(51) IPC: B 62 D 37/00 61/04

(72) Inventors: Kazuo Yamafuji

(71) Applicant: CKD K.K., et al.

(54) ATTITUDE CONTROLLING METHOD IN COAXIAL TWO WHEELER

SPECIFICATIONS /607*

1. Name of invention

Attitude controlling method in coaxial two wheeler

2. Claim

[1] With a coaxial two wheeler comprised of a pair of wheels (2, 3), axle (1) between the wheels (2, 3), car body (4) rotationally supported on the axle (1), wheel driving motor (7) mounted on the car body (4), microcomputer (16) for controlling the wheel driving motor (7), and angle detection device (11) for detecting the angle of the car body (4);

the slanted angle (Θ1) of the car (4) detected by the angle detection device (11) is sampled at short intervals (Δt); the sampled angle (Θ1) of the car body (4) used as conditional variables and feedback gain (K) used as a coefficient are respectively entered into the computer (16) to substitute and compute the pre-established input computation equation (60) to generate a control torque (T3) for the motor (7); and the computer (16) controls the motor (7) according to the computed control torque (T3).

[2] With a coaxial two wheeler comprised of a pair of wheels (2, 3), axle (1) between the wheels (2, 3), car body (4) rotationally supported on the axle (1), wheel driving motor (7) mounted on the car body (4), microcomputer (16) for controlling the wheel driving motor (7), primary angle detection device (11)

* Numbers in the margin indicate pagination in the foreign text.

for detecting the angle of the car body (4), and secondary detection device (14) for detecting the rotational angle of the wheels (2, 3);

the slanted angle (Θ1) of the car (4) detected by the primary angle detection device (11) and rotational angle (Θ3) of the wheels (2, 3) detected by the secondary detection device (11) are sampled at short intervals (Δt); the sampled angles (Θ1) of the car body (4), sampled rotational angle (Θ3) of the wheels (2, 3), and angle speed ($\dot{\Theta}1$, $\dot{\Theta}3$) computed based on those sampled angles (Θ1, Θ3) are entered into the computer (16) as conditional variables. Those values (Θ1, Θ3, $\dot{\Theta}1$, $\dot{\Theta}3$) and feedback gains ($\vec{K1}$, $\vec{KT}$) used as coefficients are substituted in the pre-stored control equations (10, 49, 51) stored in the computer (16); a control torque (T3) of the motor (7) is computed based on this computation; the motor (7) is operated by the computer (16) according to the computed torque (T3). /608

[3] With a coaxial two wheeler comprised of a pair of wheels (2, 3), axle (1) between the wheels (2, 3), car body (4) rotationally supported on the axle (1), attitude control arm (6) slantingly clamped to the car body (4), wheel driving motor (7) mounted on the car body (4), attitude control arm driving motor (9) mounted on the car body (4), microcomputer (16) for controlling the wheel driving motor (7) and attitude control arm driving motor (9), primary angle detection device (11) for

detecting the angle of the car body (4), secondary detection device (14) for detecting the rotational angle of the wheels (2, 3), and third detection device (15) for detecting the attitude control arm angle (6);

the slanted angle (Θ1) of the car (4) detected by the primary angle detection device (11), rotational angle (Θ3) of the wheels (2, 3) detected by the secondary detection device (11), and attitude control arm angle (Θ2) detected by the third detection device (15) are sampled at short intervals (Δt); using the sampled angles (Θ1) of the car body (4), rotational angle (Θ3) of the wheels (2, 3), slanted angle (Θ2) of the attitude control arm (6), and angle speed (Θ1, Θ3, Θ2) computed based on the sampled angles (Θ1, Θ3) as conditional variables and feedback gains ($\vec{K}i$, $\vec{K}t$) as coefficients, those values (Θ1, Θ3, Θ2, Θ1, Θ3, Θ2) are substituted in the pre-entered control equations (20, 49, 51) stored in the computer (16); control torques (T3, T2) for the wheel driving motor (7) and attitude control arm driving motor (9) are computed based on the values obtained from the equation computation, and the computer (16) controls the wheel driving motor (7) and attitude control arm driving motor (9) according to the control torques (T3, T2).

3. Detailed explanation of this invention

[Industrial field]

This invention pertains to an attitude controlling method for a coaxial two wheeler.

[Conventional technology]

A coaxial two wheel vehicle having wheels at both ends of one axis can be made into more compact flat shape type device compared with a four wheel or three wheel car. However, it is not practically usable unless its attitude is stably controlled. Therefore, an attitude control method was developed, in which a control arm is hung from the car body supported on the drive shaft of the coaxial two wheeler to control the angle of the control arm against a car body.

[Problems to be solved by this invention]

However, with the attitude control method which drives a control arm in the direction opposite to the slanting direction of a car, not only does this method create a control delay caused by non-linear elements (e.g., non-sensitive area of the control arm driving motor, back-rash of the gear-transmission system, etc.), but also it is unable to eliminate the noise in the angle computation performed based on the short-interval sampling of car angles and control arm angles. Therefore, stable controlling on the car attitude using an actual feedback control is difficult.

[Constituents of this invention]

[Method to solve the problems]

With the first claim of this invention, the tilt angle of a car detected by the first angle detection device is sampled at short intervals, and the control torque for the wheel driving motor is computed based on the sampled data, and the feedback control is performed on the wheel driving motor based on the

/609

computed control torque. As a result, this makes the wheels to move in the slant direction of the car to provide a recovery moment to the car. With this method, despite the fact that the control torque is immediately computed from the sampled slant angles of the car, sufficient stable attitude control can be provided.

With the second claim of this invention, the tilt angle of a car detected by the first angle detection device and wheel rotation angle detected by the secondary angle detector are sampled at short intervals, and the angle speed of those angles are computed. The control torque for the wheel driving motor is computed based on the sampled values and computed angle speeds to control the wheel driving motor using a feedback technique. As a result, the wheels can be operated in the slant direction of the car body to provide a recovery moment to the car. With this method, the use of angle speed computed from the sampled angles of the wheel and car body can further improve the attitude stability control. /610

In the third claim of this invention, the tilt angle of a car detected by the first angle detector, wheel rotation angle detected by the secondary angle detector, and slant angle of the attitude control arm detected by the third angle detector are sampled at short intervals. Control torques for the wheel driving motor and attitude control arm driving motor are computed from the sampled values to control the wheel driving motor and attitude control arm driving motor using a feedback technique.

As a result, while the wheels are operated in the slant direction of the car body, the control arm rotates in the direction opposite to the slant direction of the car to provide a recovery moment to the car. With this method, the use of an attitude control arm can provide more improved control over the wheels and car body than the first and second methods.

[Operational example]

The following explains the operational examples of this invention while referring to the figures.

As shown in Figure 1, a pair of wheels (2, 3) are attached to both ends of an axle (1) and, in turn, a square frame-form car body (4) is tiltably supported on this axle (1). A fulcrum shaft (5) is rotating installed and supported in an upper part of the car body (4), and in the center of the fulcrum shaft (5), an attitude control arm (6) with a weight (6a) is slantably clamped thereto. A reciprocally rotatable car driving motor (7) is mounted on the car (4) immediately below the weight (6a). As shown in Figure 2, a deceleration gear array (8) is positioned between the driving shaft (7a) of the motor (7) and car axle (1), allowing the decelerated rotation of the wheel driving motor (7) to be transmitted to the wheel axle (1) to make the wheels (2, 3) reciprocatingly rotate. A reciprocatingly rotatable attitude control arm driving motor (9) is mounted on the car (4) immediately above the shaft (5), an array of decelerating gears (10) are placed between the driving shaft (9a) of the motor (9) and shaft (5). With this structure, the decelerated rotation of

the attitude control arm driving motor can be transmitted to the shaft (5) to guide the attitude control arm (6) in the backward/forward directions.

The primary rotary encoder (11) is attached to the side surface of the car (4), and the rotational shaft (11a) is placed on the extension line of the axil (1). A pair of contact pieces (12, 13) are diagonally mounted onto the rotational shaft (11a), and the tips of the pieces (12, 13) contact and engage onto the floor. With this structure, the tilt angle of the car (4) to a vertical line can be detected. The secondary rotary encoder (14) is mounted onto the wheel driving motor (7), and the third rotary encoder (15) is mounted onto the attitude control arm driving motor (9), detecting each turning angle of these wheels (2, 3) and a tilt angle to a vertical line.

A microcomputer (16) for controlling the system is mounted at the lower area of the car body (4), and the detection signals transmitted from each rotary encoders (11, 14, 15) are inputted into the microcomputer (16) which computes the control torques for the wheel driving motor (7) and attitude control arm driving motor (9) on the basis of these inputted signals, thus the motors (7, 9) can be controlled with the force equivalent to the control torques. [1] Figure 3 shows the dynamic model of the simplified system exhibited in Figure 2. A wheel area (17) composed of a wheel part (19) consisting of an axle (1) and wheels (2, 3), motors (7, 9) supported by the car body (4), control computer (15), and car body (4), is expressed as a "material point" at a

distance ($\ell 1$) from the axle (1); and an arm area (18) composed of an attitude control arm (6) and weight (6a) is expressed as a "material point" at a distance ($\ell 2$) from the shaft (5). The wheel part (19) is considered to have the center of gravity on the axle (1), and the distance between the axle (1) and shaft (5) is ℓ.

The motion energy (Ko) of the dynamic model is a total of motion energy (K1) of the car body (17), motion energy (K2) of the arm part (18), and motion energy of the wheel part (19). The following describes the expression of each motion energy (K1, K2, K3) using the coordinate elements of the x-y coordinate shown in Figure 2 where the mass of the car body (17) is expressed as m1, the mass of the arm part (18) is expressed as m2, and the mass of wheel part (19) is expressed as m3:

$$K1 = (1/2)\, m1(\dot{x}1^2 + \dot{y}1^2)$$

$$K2 = (1/2)\, m2(\dot{x}2^2 + \dot{y}2^2)$$

$$K3 = (1/2)\, m_3\dot{x}3^2$$

where x and y designate the first level of differential of x and y. /611

When the tilts of the car part (17) and arm part (18) to a diagonal line are expressed as $\Theta 1$ and $\Theta 2$; the rotational angle of the wheel part (19) is expressed as $\Theta 3$; the semi-diameter of the wheels (2, 3) is expressed as r; inertia moment in the direction of axle (1) of the car part (17) is expresses as J1; and inertia moment in the direction of shaft (5) of the arm part (18) is expresses as J2; the following expressions are formed:

$$K_1 = (1/2)\, m_1 \times \{ (r\dot{\theta}_3 + \ell\dot{\theta}_1 \cdot \cos\theta_1)^2 + \ell_1^2\theta_1^2 \cdot \sin^2\theta_1 \}$$
$$= (1/2)\, m_1 \times (r^2\dot{\theta}_3^2 + 2 r \ell_1 \dot{\theta}_3 \dot{\theta}_1 \cdot \cos\theta_1 + \ell_1^2\dot{\theta}_1^2)$$
$$= (1/2)\, m_1 r^2 \dot{\theta}_3^2 + m_1 r^2 \ell_1 \dot{\theta}_3 \dot{\theta}_1 \cdot \cos\theta_1 + (1/2)\, J_1 \dot{\theta}_1^2$$

$$K2 = (1/2)\, m_2 \times \{ (r\dot{\theta}_3 + \ell\dot{\theta}_1 \cdot \cos\theta_1 - \ell_2\dot{\theta}_2 \cdot \cos\theta_2)^2 + (-\ell\dot{\theta}_1 \cdot \sin\theta_1 - \ell_2\dot{\theta}_2 \cdot \sin\theta_2)\}$$
$$= (1/2)\, m_2 r^2 \dot{\theta}_3^2 + m_2 r \dot{\theta}_3 (\ell\dot{\theta}_1 \cdot \cos\theta_1 - \ell_2\dot{\theta}_2 \cdot \cos\theta_2) - m_2 \ell \ell_2 \dot{\theta}_1 \dot{\theta}_2 \cdot \cos(\theta_1 - \theta_2)$$
$$+ (1/2)\, m_2 \ell^2 \dot{\theta}_1^2 + (1/2)\, J_2 \dot{\theta}_2^2$$

$$K3 = (1/2)\, m_3 r^2 \dot{\theta}_3^2$$

where Θ1, Θ2, and Θ3 are the first-level differential of Θ1, Θ2, and Θ3.

As for the motion energy (K_3) of the wheel part (19), rotational energy based on the inertia moment in the direction of the center of the gravity exists. When the inertia moment is designated as J_3, the movement energy (K_3) can be expressed as below:

$$K3 = (1/2)\, m3\, r^2\Theta3^2 + (1/2) J3\, \Theta3^2$$

Therefore, the motion energy (K) can be expressed as below:

$$K_0 = K_1 + K_2 + K_3$$
$$= (1/2) \cdot (J_1 + m_2 \ell^2)\dot{\theta}_1^2 + (1/2)\, J_2 \dot{\theta}_2^2 + (1/2) \cdot (m_1 r^2 + m_2 r^2 + m_3 r^2 + J_3)\dot{\theta}_3^2$$
$$- m_2 \ell_2 \ell \dot{\theta}_1 \dot{\theta}_2 \cdot \cos(\theta_1 - \theta_2) + (m_2 \ell_1 + m_2 \ell) r \dot{\theta}_1 \dot{\theta}_3 \cdot \cos\theta_1 - m_2 \ell_2 r \dot{\theta}_2 \dot{\theta}_3 \cdot \cos\theta_2 \quad \cdots (1)$$

The positional energy (P) can be expressed as below when the gravity acceleration ratio is expressed as g:

$$P = (m_1 \ell_1 + m_2 \ell) g \cdot \cos \theta_1 - m_2 \ell_2 g \cdot \cos \theta_2 \quad \cdots (2)$$

The energy loss (D) can be expressed as below when the viscous friction coefficients of car-part motion (17), arm-part motion (18), and wheel-part rotation (19) are respectively expressed as f_1, f_2, and f_3:

$$D = (1/2) f_2 \dot{\theta}_2^2 + (1/2) f_3 \dot{\theta}_3^2 \quad \cdots (3)$$

Since the torques (T2, T3) respectively exist for the arm part (18) and wheel part (19), a Lagrange motion equation described below can be established:

$$d/dt * \delta/\delta \dot{\theta}_i * K - \delta/\delta \theta_i * K + \delta/\delta \theta_i * P + \delta/\delta \dot{\theta}_i * D = T_i \quad (i = 1, 2, 3) \quad \cdots (4)$$

where d/dt is an ordinary differential equation, and $\delta/\delta\Theta i$ and $\delta/\delta\Theta i$ are a partial differential equation.

By substituting equations (1), (2), and (3) in Equation (4), and once Equation (4) is organized, the following equations can be established:

$$A_1 \ddot{\theta}_1 + B_1 \cdot \cos (\theta_1 - \theta_2) \ddot{\theta}_2 + C_1 \cdot \cos \theta_1 \ddot{\theta}_3 + D_1 \cdot \sin (\theta_1 - \theta_2) \dot{\theta}_2^2 + E_1 \cdot \sin \theta_1 + f_1 \dot{\theta}_1 = 0 \quad \cdots (5)$$

$$B_1 \cdot \cos (\theta_1 - \theta_2) \ddot{\theta}_1 + B_2 \ddot{\theta}_2 + C_2 \cdot \cos \theta_2 \ddot{\theta}_3 + D_2 \cdot \sin (\theta_1 - \theta_2) \dot{\theta}_1^2 + E_2 \cdot \sin \theta_2 + f_2 \dot{\theta}_2 = T_2 \quad \cdots (6)$$

$$C_1 \cdot \cos\theta_1 \ddot{\theta}_1 + C_2 \cdot \cos\theta_2 \ddot{\theta}_2 + C_3 \ddot{\theta}_3 + D_3 \cdot \sin\theta_1 \dot{\theta}_1^2 + E_3 \cdot \sin\theta_2 \dot{\theta}_2^2 + f_3 \dot{\theta}_3 = T_3 \quad \cdots (7)$$

where

$$A_1 = J_1 + m_2 \ell^2$$

$$B_1 = -m_2 \ell^2 \ell$$

$$C_1 = (m_1 \ell + m_2 \ell)r$$

$$D_1 = -m_2 \ell^2 \ell$$

$$E_1 = -(m_1 \ell_1 + m_2 \ell)g$$

$$B_2 = J_2$$

$$C_2 = -m_2 \ell^2 r$$

$$D_2 = -m_2 \ell^2 \ell$$

$$E_2 = -m_2 \ell^2 g$$

$$C_3 = (m_1 + m_2 + m_3)r^2 J_3$$

$$D_3 = -(m_1 \ell + m_2 \ell)r$$

$$E_3 = -m_2 \ell_2 r$$

[2] Next, the following explains the design of the linear type control system for the dynamic model shown in Figure 3:

The following approximation is performed under the assumption that the dynamic model shown in Figure 3 is consistently controlled so that Θ1 and Θ2 never become excessively high values.

$$\sin\theta_1 \fallingdotseq \theta_1 \qquad \sin\theta_2 \fallingdotseq \theta_2$$

$$\cos\theta_1 = \cos\theta_2 = \cos(\theta_1 - \theta_2) \fallingdotseq 1$$

$$\sin\theta_2 \dot{\theta}_2^2 = \sin(\theta_1 - \theta_2)\dot{\theta}_1^2 = \sin(\theta_1 - \theta_2)\dot{\theta}_2^2 = 0$$

Based on this approximation, the equations (5), (6), and (7) can be made into the following linear equations:

$$\ddot{\theta}_1 = A_{11}\theta_1 + A_{12}\theta_2 + A_{13}\dot{\theta}_1 + A_{14}\dot{\theta}_2 + B_{11}T_2 \quad \cdots (8)$$

$$\ddot{\theta}_2 = A_{21}\theta_1 + A_{22}\theta_2 + A_{23}\dot{\theta}_1 + A_{24}\dot{\theta}_2 + B_{21}T_2 \quad \cdots (9)$$

where

$$A_{11} = E_1 B_2/\Delta \qquad A_{12} = -E_2 B_1/\Delta$$
$$A_{13} = f_1 B_2/\Delta \qquad A_{14} = -f_2 B_1/\Delta$$
$$A_{21} = -E_1 B_1/\Delta \qquad A_{22} = -E_2 A_1/\Delta$$
$$A_{23} = -f_1 B_1/\Delta \qquad A_{24} = -f_2 A_1/\Delta$$
$$B_{11} = B_1/\Delta \qquad B_{21} = -A_1/\Delta$$
$$\Delta = B_1^2 - A_1 B_2$$

Assuming that x1 = Θ1, x2 = Θ2, x3 = Θ1, and x4 = Θ2, the following vector and matrix display are performed:

$$\vec{X} = \begin{bmatrix} x_1 \\ x_2 \\ x_3 \\ x_4 \end{bmatrix} \quad \overline{A} = \begin{bmatrix} 0 & 0 & 1 & 0 \\ 0 & 0 & 0 & 1 \\ A_{11} & A_{12} & A_{13} & A_{14} \\ A_{21} & A_{22} & A_{23} & A_{24} \end{bmatrix}$$

$$\vec{B} = \begin{bmatrix} 0 \\ 0 \\ B_{11} \\ B_{21} \end{bmatrix} \quad \overline{C} = \begin{bmatrix} 1 & 0 & 0 & 0 \\ 0 & 1 & 0 & 0 \end{bmatrix}$$

$$u = T_2$$

The following conditional equation and output equation can be obtained using the vector and matrix display described above:

$$\dot{\vec{X}}(t) = \overline{A} \cdot \vec{X}(t) + \vec{B} \cdot u(t) \quad \cdots (10)$$

$$\vec{Y}(t) = \overline{C} \cdot \vec{X}(t) \quad \cdots (11)$$

By Laplace-transforming the conditional equation (10), the following equation can be established:

$$\int_0^{\infty} \dot{\vec{X}}(t)\, e^{-st}\, dt$$

$$= \int_0^{\infty} \vec{X}(t)\, e^{-st}\, dt + s \int_0^{\infty} \vec{X}(t)\, e^{-st}\, dt$$

$$= s\vec{X}(s) = \overline{A} \cdot \vec{X}(s) + \vec{B} \cdot u(s)$$

Therefore,

$$\vec{X}(s) = (s\overline{I} - \overline{A})^{-1} \vec{B} \cdot u(s) \quad \cdots (12)$$

where $\overline{I}$ is a unit matrix, $(s\overline{I} - \overline{A})^{-1}B$ is a reversed matrix of $(s\overline{I} - \overline{A})$.

By substituting the equation (12) in the output equation (11), the following equation can be established: /613

$$\vec{Y}(s) = \overline{C}(s\overline{I} - \overline{A})\vec{B} \cdot u(s) \quad \cdots (13)$$

The function expressed as $\vec{Y}(s)/u(s)$ is called "transfer function" based on the control theory, and is expressed as the following polynomial equation:

$$\frac{\vec{Y}(s)}{u(s)} = k\,\frac{(s-\sigma_1)(s-\sigma_2)(s-\sigma_3)(s-\sigma_4)}{+(s-\lambda_1)(s-\lambda_2)(s-\lambda_3)(s-\lambda_4)} \quad \cdots (14)$$

$(s - \lambda 1)$, $(s - \lambda 2)$, $(s - \lambda 3)$, and $(s - \lambda 4)$ in Equation (14) are characteristic polynomial equations, k is a gain, and λi (i = 1, 2, 3, 4) is called "pole". When the pole λi exists on the right half of the complex variable plane, that is, the real values are positive, the system expressed with equations (10) and

(11) is known to be unstable; whereas when the pole λi exists on the left half of the complex variable plane, that is, the real values are negative, the system expressed with equations (10) and (11) is known to be stable. For example, when the system parameters of the dynamic model shown in Figure 3 are the following values, the pole is confirmed to exist on the right half on the complex plane.

$m_1 = 2.59$ Kg $\quad \ell = 0.318$ m

$m_2 = 1.52$ Kg $\quad \ell = 0.17$ m

$m_3 = 0.36$ Kg $\quad \ell = 0.20$ m

$J_1 = 0.108$ Kgm

$J_2 = 7.01 \times 10$ Kgm

$J_3 = 5.00 \times 10$ Kgm

$r = 4.5 \times 10^{-2}$m

$f_1 = 6.0 \times 10$ Nms

$f_2 = 4.40 \times 10$ Kgm

$f_3 = 4.40 \times 10$ Kgm

In order to stabilize the dynamic model shown in Figure 3, the control input u(t) must be added to transfer the unstable condition to the stable condition. To achieve this, the existence of u(t) must be guaranteed. If u(t) exists, the dynamic model expressed as Expressions (10) and (11) is controllable. It is a known factor based on the control theory that the necessary/sufficient condition is that the ranks $[\vec{B}, \vec{AB}, \vec{A^2B}, \vec{A^3B}]$ of a matrix called controllable matrix match the

conditional variables (x1, x2, x3, x4). The system expressed with equations (10) and (11) is controllable as it satisfies this necessary/sufficient condition.

To transform the system expressed as equations (10) and (11) to the system to which conditional feedback control is added, the following equation is used:

$$\vec{u}(t) = -\vec{K} \cdot \vec{X}(t) + c\vec{V}(t) \quad \cdots (15)$$

where $\vec{K}$ is a vector called conditional feedback gain, and c is a scaler.

By substituting the equation (15) in equations (10) and (11), the following conditional equation and output equation can be obtained:

$$\dot{\vec{X}}(t) = (\overline{A} + \vec{B}\vec{K})\vec{X}(t) + c\vec{B} \cdot \vec{V}(t) \quad \cdots (16)$$

$$\vec{Y}(t) = \overline{C} \cdot \vec{X}(t) \quad \cdots (17)$$

By Laplus-transforming the conditional equation (16), the following equation can be made:

$$\vec{X}(s) = (s\overline{I} - \overline{A} - \vec{B}\vec{K})\, c\vec{B} \cdot \vec{V}(s) \quad \cdots (18)$$

By substituting equation (18) to the output equation (17), the following equation can be made:

$$\vec{Y}(s) = \overline{C}(s\overline{I} - \overline{A} - \vec{B}\vec{K})\, c\vec{B} \cdot \vec{V}(s) \quad \cdots (19)$$

Therefore, inherent polynomial of the matrix $(\bar{A} + \vec{\vec{BK}})$ matches

the characteristic polynomial, thereby the inherent value of matrix $(\bar{A} + \vec{\vec{BK}})$ agree with the pole.

It is an established factor based on the control theory that /614 equations (16) and (17) must be controllable for matching the characteristic polynomial expressed as equation (19) with Monique polynomial [i.e., necessary/sufficient condition for optionally establishing the inherent value of matrix $(\bar{A} + \vec{\vec{BK}})$]. Therefore, by appropriately establishing the conditional feedback gain $\vec{K}$, the system can be stabilized by positioning a pole at an appropriate location in the right half of the complex plane.

When c = 0, the conditional equation (16) designating the controllable system shown in Figure 3 is expressed as below:

$$\dot{\vec{X}}(t) = (\bar{A} + \vec{B}\vec{K})\vec{X}(t)$$

that is,

$$\vec{u}(t) = \vec{K} \cdot \vec{X}(t) \quad \cdots (20)$$

The feedback gain $\vec{K}$ in equation (20) can be obtained by the following method:

(1) Select preferable four different and symmetrical poles Si (i = 1, 2, 3, 4).

(2) Compute the following equation after selecting the real number (gi) when all the poles (Si) are real numbers.

$$Fi = (Si \cdot \overline{I} - \overline{A}) \vec{Bgi}$$

(3) When all the poles (Si) are complex numbers $\alpha + \beta j$ (j is an imaginary number), Si + 1 is made into a conjugate root $\alpha 1 - \beta i$ j, and appropriate real numbers gi, gi+ 1 are selected, then, the following equations are computed:

$$f_1 = \{ (\alpha_1 \overline{I} - \overline{A}) \vec{B} g_{1+} \beta_1 \vec{B} g_{1+1} \} + \{ (\alpha_1 \overline{I} - \overline{A})^2 + \beta_1^2 \overline{I} \}$$

$$f_{1+1} = \{ (\alpha_1 \overline{I} - \overline{A}) \vec{B} g_{1+1} + \beta_1 \vec{B} g_1 \} + \{ (\alpha_1 \overline{I} - \overline{A})^2 + \beta_1^2 \overline{I} \}$$

With those computations, the feedback gain $\vec{K}$ becomes the following:

$$\vec{K} = [g_1, g_2, g_3, g_4] \begin{bmatrix} f_1 \\ f_2 \\ f_3 \\ f_4 \end{bmatrix} = [g_1, g_2, g_3, g_4] [f_1, f_2, f_3, f_4]^T \quad \cdots (21)$$

[3] In special cases of the dynamic model shown in Figure 3, that is, the coaxial two wheelers from which the attitude control arm (6) is removed (shown in Figure 4 and its dynamic model is shown in Figure 5). The Lagrange motion equation of the dynamic model shown in Figure 5 can be obtained by the following equation using equations (5), (6), and (7):

$$A_1 \ddot{\theta}_{1+} C_1 \cdot \cos \theta_1 \ddot{\theta}_{3+} E_1 \cdot \sin \theta_1 + f_1 \dot{\theta}_1 = 0 \quad \cdots (22)$$

$$C_1 \cdot \cos \theta_1 \ddot{\theta}_{1+} C_3 \ddot{\theta}_3 + D_3 \cdot \sin \theta_1 \dot{\theta}_1^{2+} f_3 \dot{\theta}_3 = T_3 \quad \cdots (23)$$

The following approximation is performed with the equations (8) and (9):

$$\sin\theta_1 \approx \theta_1 \qquad \cos\theta_1 \approx 1 \qquad \sin\theta_3 \approx \theta_3$$

With this approximation, equations (22) and (23) are linear-processed as described below:

$$\ddot{\theta}_1 = A_{11}\theta_1 + A_{13}\dot{\theta}_1 + A_{14}\dot{\theta}_3 + B_{11}T_3 \qquad \cdots (24)$$

$$\ddot{\theta}_3 = A_{21}\theta_1 + A_{23}\dot{\theta}_1 + A_{24}\dot{\theta}_3 + B_{21}T_3 \qquad \cdots (25)$$

where

$A_{11} = E_1 C_3/\Delta$ $\quad A_{13} = -f_1 C_3/\Delta$

$A_{14} = f_3 C_1/\Delta$ $\quad A_{21} = E_1 C_1/\Delta$

$A_{23} = f_1 C_1/\Delta$ $\quad A_{24} = -f_3 A_1/\Delta$

$B_{11} = -C_1/\Delta$ $\quad B_{21} = A_1/\Delta$

$E_1 = -m_1 g \ell_1$ $\quad C_1 = m_1 \ell_1 r$

$C_3 = (m_1+m_3) r^2 + J_3$ $\quad A_1 = J\hat{1}$

$\Delta = A_1 C_3 - C_3^2$

Assuming that x1 = Θ1, x2 = Θ3, x3 = Θ1, and x4 = Θ3, the following vector and matrix display are performed:

$$\vec{X} = \begin{pmatrix} x_1 \\ x_2 \\ x_3 \\ x_4 \end{pmatrix} \quad \overline{A} = \begin{pmatrix} 0 & 0 & 1 & 0 \\ 0 & 0 & 0 & 1 \\ A_{11} & A_{12} & A_{13} & A_{14} \\ A_{21} & A_{22} & A_{23} & A_{24} \end{pmatrix}$$

$$\vec{B} = \begin{pmatrix} 0 \\ 0 \\ B_{11} \\ B_{21} \end{pmatrix} \quad \overline{C} = \begin{pmatrix} 1 & 0 & 0 & 0 \\ 0 & 1 & 0 & 0 \end{pmatrix}$$

u = T3 /615

Using those vector and matrix display, the following conditional equation and output equation can be obtained:

$$\dot{\vec{X}}(t) = \overline{A} \cdot \vec{X}(t) + \vec{B} \cdot u(t) \quad \cdots (26)$$

$$\vec{Y}(t) = \overline{C} \cdot \vec{X}(t) \quad \cdots (27)$$

Parts (a) and (b) in Figure 6 show the computer simulation results for the equations (26) and (27) using the feedback gain $\vec{K}$ expressed as expression (21) established according to the methods (1) ~ (3) described above. With those simulations, the numeric value differentiation method described later is used. In Part (a) in Figure 6, curve (C1) shows the variation of the tilted angle ($\Theta 1$) of the car body part (17), and curve (C2) shows the variation of the rotational angle ($\Theta 3$) of the wheel part (19). In Part (b) in Figure 6, curve (C3) shows the variation of the tilted angle speed ($\Theta 1$) of the car body part (17); curve (C4) shows the variation of the rotational angle speed ($\Theta 3$) of the wheel part (19). The parameters and conditions are established as following:

$m_1 = 2.79$ kg $\quad \ell = 0.318$ m
$m_2 = 0$ kg $\quad \ell_1 = 0.19$ m
$m_3 = 0.36$ kg $\quad \ell_2 = 0$ m
$J_1 = 0.12237$ kgm
$J_2 = 0$ kgm
$J_3 = 5.00 \times 10$ kgm
$r = 4.5 \times 10^{-2}$ m
$f_1 = 6.86 \times 10$ Nms
$f_2 = 0$ Nms
$f_3 = 4.40 \times 10$ Nms
$Si = (-5 \pm 4j, -6 \pm 5j)$
$(i = 1, 2, 3, 4)$

$\vec{K} = [4.88, 1.31, 5.37, 6.00]$
$\vec{X}(0) = [0, 0, \pi/10, 0]$

Note that $\vec{X}(0) = [0.0, \pi/10.0]$ expresses the initial condition; disturbance $\pi/10$ (rad/s) is provided to the car part (17); and 5 ms is used as simulation interval Δt. The simulation results shown in Parts (a) and (b) in Figure 6 indicate that the car part (17) can be returned to the balanced position ($\Theta 1 = 0$) shown in Figure 4 and maintained thereafter. Also, with this balancing control, although the further the pole positioned to the right half of the complex plane, the greater the control input becomes, the control system can be quickly stabilized.

[4] With the dynamic models expressed as equations (22) and (23), assuming that the attitude control arm (6) is removed and the wheels (1) are almost stand still to ignore the motion related to the wheels (1) and approximation of $\sin \Theta 1 \approx \Theta 1$ is performed, the following motion equation can be established:

$$A_1 \ddot{\theta}_1 + f_1 \dot{\theta}_1 + E_1 \cdot \sin\theta_1 - J_1 \ddot{\theta}_1 + f_1 \dot{\theta}_1 - m_1 g \ell \theta_1 = 0 \quad \cdots (59)$$

Feedback of u(t) = T3 is provided to the system expressed as Equation (59).

$$J_1 \ddot{\theta}_1 + f_1 \dot{\theta}_1 - m_1 g \ell \theta_1 = u(t) = -\xi K \theta_1 (t) \quad \cdots (60)$$

Note that this is a constant determined by the torque function of the wheel driving motor (7), deceleration ratio of driving system, etc.

Considering the overall control delay time ΔT [e.g., detection of tilt angle $\Theta 1$, computation time by the computer (16), command input time for wheel driving motor (7), transfer delay by the deceleration gears (8), etc.], the equation (60) becomes the following:

$$J_1 \ddot{\theta}_1 + f_1 \dot{\theta}_1 - m_1 g \ell \theta_1 = -\xi K \theta_1 (t - \Delta T) \quad \cdots (61)$$

By Taylor-developing $\Theta 1(t - \Delta T)$ while ignoring the two dimensional small values, the following equation is made:

$$\theta_1 (t - \Delta T) \fallingdotseq \theta_1(t) - \Delta T \dot{\theta}_1(t)$$

/616

As a result, equation (61) becomes the following:

$$J_1 \ddot{\theta}_1 + (f_1 - K \xi \Delta T) \dot{\theta}_1 + (K \xi - m_1 g \ell) \theta_1 = 0 \quad \cdots (62)$$

The following characteristic equation can be obtained by Laplus-transforming the equation (62):

$$J_1 s^2 + (f_1 - K \xi \Delta T) s + (K \xi - m_1 g \ell) = 0 \quad \cdots (63)$$

The stabilization condition for the control system expressed as equation (63) can be obtained as below based on the Routh-Hurwitz stabilization conditions:

$$m_1 g \ell / \xi < K < \xi \Delta T \quad \cdots (64)$$

With equation (64), although the lower limit of the feedback gain K is fixed, the upper limit varies depending on the delay time ΔT. That is, smaller the ΔT is, the greater the selection range of feedback gain becomes, and the selectability of appropriate feedback gain K becomes higher.

The computer simulation result performed on equation (62) using feedback gain K selected from equation (64) exhibits the attitude stability control equal to the stable attitude stability provided to the linear control system described above (refer to [3]). For example, the attitude stability is excellent when ΔT = 3ms and K = 10.0.

Also, the experiment results on the control system expressed as equation (62) confirm that no negative results occur with the use of sampling time Δt when the delay time is ΔT.

[5] The feedback controls described above are all based on the polar position method. The following explains the feedback control using an optimal control method:

The control system shown in Figure 3 is expressed as equation (10):

$$\dot{\vec{X}}(t) = \overline{A} \cdot \vec{X}(t) + \vec{B} \cdot u(t) \quad \cdots (10)$$

The control input u(t) is then determined from equation (10) to minimize the evaluation function J(u):

$$J(u) = \int_0^{\infty} \left(\vec{X}^T(t) \, \overline{Q} \cdot \vec{X}(t) + u^T(t) \, R \, U(t) \right) dt \quad \cdots (28)$$

where $\bar{Q}$ and R are respectively 4 x 4 and 1 x 1 absolute symmetric matrixes. By minimizing J(u) as much as possible, the initial condition can be maximally stabilized with a small control energy. The optimal input uo(t) which minimizes J(u) can be obtained as equation (31) from the solution $\bar{P}$ of the Riccati equation (29):

$$\bar{A}^{T}\bar{P} + \bar{P}\bar{A} - \bar{P}\vec{B}R^{-1}\vec{B}\bar{P} + \bar{Q} = 0 \quad \cdots (29)$$

$$\vec{K} = -R^{-1}\vec{B}\bar{P} \quad \cdots (30)$$

$$u_0(t) = -\vec{K}\cdot\vec{X}(t) \quad \cdots (31)$$

Therefore, by obtaining $\vec{K}$, the optimum input uo(t) can be produced in the form of feedback.

The feedback gain $\vec{K}$ for the conditional equation (16) expressing the controllable system shown in Figure (3) can be obtained in the following manner:

(1) Appropriate diagonal matrix $\bar{Q}$ and R are selected.

(2) $\vec{K}$ (i = 0) is selected to stabilize $\bar{A} + \vec{\vec{B}}\vec{K}$ ($\vec{K}$ computed in the polar positioning method is used for simplification).

(3) Assuming $\bar{A}i = \bar{A} + \vec{\vec{B}}Ki$, 4 x 4 semi-absolute symmetric matrix solution $\bar{P}$ of the Lyapnov equation (32) is obtained. /617

$$\bar{A}_i^{T}\bar{P} + \bar{P}_i\bar{A}_i + \bar{Q} + \vec{K}_i^{T}R\vec{K} = 0 \quad \cdots (32)$$

(4) Return to (3) after setting $\vec{K}i+1 = -R^{-1}B^{T}Pi$ and $i = i + 1$.

By repeating those processes, the convergence value $\vec{K}$ of $\vec{K}i$ can be obtained.

The weight $\bar{Q}$ and R in the evaluation function (28) strongly affect the control capability of the control system, and according to the results of experiments conducted by the developer of this invention, smaller the ratio of R to $\bar{Q}$ is, the faster the controlling speed becomes. Also, with the dynamic mode shown in Figure 3, since the stability of the car part (17) is more important than stability of the arm part (18), $\bar{Q}$ must be delibe-rately selected so that greater weight can be placed to the diagonal element of Q corresponding to X1. For this reason, the optimum control method is better than the polar positioning method. As described with the simulation result obtained with the polar positioning method, The simulation result obtained from the optimum control method returns the car part (17) to the balanced position ($\Theta 1 = 0$) (see a broken line in Figure 4), and the balanced condition can be maintained thereafter.

[6] The following explains the design of a non-linear type control system of the dynamic model shown in Figure 3:

With the linear type control system, an assumption was made that the dynamic model shown in Figure 3 was constantly controlled to prevent excessive $\Theta 1$ and $\Theta 2$. With the non-linear type control system, the following assumptions are made:

(1) The slant angle $\Theta 1$ of the car part (17) is controlled so that it does not become excessively high.

(2) The rotational acceleration speed Θ3 of the wheel part (19) is extremely narrow.

(3) When the slant angle Θ1 of the car part (17) is wide, the angle speed Θ1 is narrow.

(4) When the slant angle Θ2 of the arm part (18) is wide, the angle speed Θ1 is narrow.

(5) When the angle speed Θ1 of the car part (17) is wide, the slant angle Θ1 is narrow.

(6) When the angle speed Θ2 of the arm part (18) is wide, the slant angle Θ2 is narrow.

With those assumptions (1 ~ 6), equations (5), (6), and (7) expressing the dynamic model shown in Figure 3 can be simplified as described below:

$$A_1 \ddot{\theta}_1 + B_1 \cdot \cos\theta_2 \ddot{\theta}_2 + E_1 \theta_1 + f_1 \dot{\theta}_1 = 0 \quad \cdots (33)$$

$$B_1 \cdot \cos\theta_2 \ddot{\theta}_1 + B_2 \ddot{\theta}_2 + E_2 \cdot \sin\theta_2 + f_2 \dot{\theta}_2 = T_2 \quad \cdots (34)$$

$$C_1 \ddot{\theta}_1 + C_2 \cdot \cos\theta_2 \ddot{\theta}_2 + C_3 \ddot{\theta}_3 + f_3 \dot{\theta}_3 = T_3 \quad \cdots (35)$$

$$\begin{bmatrix} \ddot{\theta}_1 \\ \ddot{\theta}_2 \end{bmatrix} = \begin{bmatrix} a & b \\ c & d \end{bmatrix} \begin{bmatrix} -E_1 \theta_1 - f_1 \dot{\theta}_1 \\ T_2 \cdot \end{bmatrix} \quad \cdots (36)$$

$$\begin{bmatrix} a & b \\ c & d \end{bmatrix} = \begin{bmatrix} A_1 & B_1 \cdot \cos\theta_2 \\ B_1 \cdot \cos\theta_2 & B_2 \end{bmatrix}^{-1} \quad \cdots (37)$$

$$T_2 ' = T_2 - E_2 \cdot \sin\theta_2 - f_2 \dot{\theta}_2 \quad \cdots (38)$$

Then, the following vector and matrix display are performed:

$$\vec{\theta} = \begin{bmatrix} \theta_1 \\ \dot{\theta}_1 \\ \theta_2 \\ \dot{\theta}_2 \end{bmatrix} \qquad \vec{B} = \begin{bmatrix} 0 \\ b \\ 0 \\ c \end{bmatrix}$$

$$\overline{A} = \begin{bmatrix} 0 & 1 & 1 & 1 \\ -aE_1 & -af_1 & 0 & 0 \\ 0 & 1 & 1 & 1 \\ -bE_1 & -bf_2 & 0 & 0 \end{bmatrix}$$

As a result, equation (34) is rewritten into the following conditional equation (39):

$$\dot{\vec{\theta}}(t) = \overline{A} \cdot \vec{\theta}(t) + \vec{B} \cdot T_2'(t) \qquad \cdots (39)$$

/618

Since $\overline{A}$ in equation (39) is a coefficient varies with the passage of time (time-variation), at least one pole is positioned at the right half of the complex plane, where the system expressed as equation (39) is known to be unstable. In order to fix the time-varying pole in the unstable system at a position in the left half of the complex plane to stabilize the system, the following feedback control is performed to the system expressed as Expression (39):

$$T_2' = [k_1, k_2, k_3, k_4][\theta_1, \theta_2, \theta_3, \theta_4]^T = -\vec{K}\vec{\theta} \qquad \cdots (40)$$

As a result, expression (39) can be made into the following equation:

$$\dot{\vec{\theta}}(t) = (\overline{A} + \vec{B}\vec{K})\vec{\theta}(t) \qquad \cdots (41)$$

The characteristic polynomial of equation (41) (i.e., the inherent polynomial equation $\overline{A} + \vec{B}\vec{K}$) becomes the following:

$$
\begin{aligned}
D(\lambda) &= det\{\lambda \overline{I} - (\overline{A} + \vec{B}\vec{K})\} \\
&= |\lambda \overline{I} - \overline{A} - \vec{B}\vec{K}| \\
&= \lambda^4 + (a f_1 - b k_2 - c k_4)\lambda^3 \\
&\quad + (a E_1 - b k_1 - c k_3 - f_1 k_4/\Delta)\lambda^2 \\
&\quad - (f_1 k_3 + E_1 k_4)\lambda/\Delta - E_1 k_3/\Delta \qquad \cdots (42)
\end{aligned}
$$

where $\Delta = ac - b^2$.

Since the poles in the system expresses as expression (41) are all assumed to be fixed, the coefficient in the equation (42) must not change with the passage of time (non-time-varying). Since $\overline{A}$ and $\vec{B}$ are time-varying coefficients, $\vec{K}$ naturally becomes time-varying. To obtain this time-varying $\vec{K}$ (from here, expressed as $\vec{Kt}$), one preferably stable linear non-time-varying model expressed as Expression (43) is selected.

$$\dot{\vec{X}}(t) = \overline{A}' \cdot X(t) \qquad \cdots (43)$$

As the control system expressed as equation (41) always agrees with equation (43) [i.e., the poles in the system expressed as equation (41) can agree with and is fixed to the poles in the system expressed as expression (43)], the control system expressed as expression (41) can be stabilized. The poles for the equation (43) are expressed as below:

$-\alpha 1 + \beta 1\, j$ ($\alpha > 0$, i = 1, 2, 3, 4)

This characteristic polynomial is expressed as below:

$$D(\lambda) = |\lambda \bar{I} - \bar{A}'|$$

$$= \begin{vmatrix} \lambda & 0 & 0 & 0 \\ 0 & \lambda & 0 & 0 \\ 0 & 0 & \lambda & 0 \\ 0 & 0 & 0 & \lambda \end{vmatrix}$$

$$- \begin{vmatrix} -\alpha_1 + \beta_1 j & 0 & 0 & 0 \\ 0 & -\alpha_2 + \beta_2 j & 0 & 0 \\ 0 & 0 & -\alpha_3 + \beta_3 j & 0 \\ 0 & 0 & 0 & -\alpha_4 + \beta_4 j \end{vmatrix}$$

$$= \lambda^4 + d_3 \lambda^3 + d_2 \lambda^2 + d_1 \lambda + d_0 \quad \cdots (44)$$

By consistently coincide the coefficient of the characteristic polynomial in equation (42) with the characteristic polynomial of the equation (43), each element (k1, k2, k3, k4) of $\vec{Kt}$ becomes the following:

$$k_1 = 1/b \cdot (a E_1 - d_2 + f_1 d_1/E_1 - c \Delta d_0/E_1 - f_1^2 d_0/E_1^2) \quad \cdots (45)$$

$$k_2 = 1/b \cdot (a f_1 - d_3 + c \Delta d_1/E_1 + f_1 c \Delta d_0/E_1^2) \quad \cdots (46)$$

$$k_3 = -\Delta d_0/E_1 \quad \cdots (47)$$

$$k_4 = (\Delta/E_1) \cdot (f_1 d_0/E_1 - d_1) \quad \cdots (48)$$

The poles in the equation (39) expressing the time-varying system produced by those computations consistently coincides with the poles ($-\alpha 1 + \beta 1 j$) of the stable linear time-varying model (41), and the feedback coefficient $\vec{Kt}$ is made into a time-varied quantity at each sampling time by equations (45) ~ (48). That is, this feedback becomes a kind of adaptation-control process, which is a model-matching process to the time-varying system parameters. /619

The control input T1 of the arm part (18) can be obtained from equation (38) by the following method:

$$T_2 = T_2' + E_2 \cdot \sin\theta_2 + f_2\dot{\theta}_2$$
$$= \vec{K}t\,\vec{\theta} + E_2 \cdot \sin\theta_2 + f_2\dot{\theta}_2 \quad \cdots (49)$$

The control input T3 for the wheel part (19) can be obtained from equation (35):

$$T_3 = c_1\ddot{\theta}_1 + c_2 \cdot \cos\theta_2\,\ddot{\theta}_2 + c_3\ddot{\theta}_3 + f_3\ddot{\theta}_3$$
$$= [c_1, c_2 \cdot \cos\theta_2] \begin{pmatrix} \ddot{\theta}_1 \\ \ddot{\theta}_2 \end{pmatrix} + f_3\dot{\theta}_3 + c_3\ddot{\theta}_3$$

By substituting equations (37) and (40), the following equation is made:

$$= [c_1, c_2 \cdot \cos\theta_2] \begin{bmatrix} a & b \\ b & c \end{bmatrix}$$
$$\times \begin{pmatrix} -E_1\theta_1 - f_1\dot{\theta}_1 \\ \vec{K}t \cdot \vec{\theta} \end{pmatrix} + f_3\dot{\theta}_3 + c_3\ddot{\theta}_3$$
$$\cdots (50)$$

By entering a control input that can approximate the angle speed Θ3 of the wheels (2, 3) close to the target angle speed Θ3, the wheels (2, 3) can be transferred at equal speed. Therefore, the control input for the wheel part (19) is expressed as below:

$$T_3 = [c_1, c_2 \cdot \cos\theta_2] \begin{bmatrix} a & b \\ b & c \end{bmatrix}$$

$$\times \begin{pmatrix} -E_1\theta_1 - f_1\dot{\theta}_1 \\ \vec{K} \cdot \vec{\theta} \end{pmatrix} + f_3\dot{\theta}_3 + c_3(\dot{\theta}_3 - \dot{\theta}_3')$$
$$\cdots (51)$$

The time-varying feedback gain $\vec{K}t$ is computed from the sampling condition quantity (Θ1, Θ2, Θ3) of each time. Parts (a), (b), and (c) in Figure 7 shows the computer simulation result performed on equation (39) using those computed values. The curves (C5, C7, C9) shown in Parts (a), (b), and (c) in Figure 7 designate the variation of the slant angle Θ1 of the car part (19), and curves (C6, C8, C10) designate the variation of the slant angle Θ2 of the arm part (18). The parameters and conditions for those simulations are the following:

$m_1 = 2.79$ kg $\quad \ell = 0.318$ m
$m_2 = 1.40$ kg $\quad \ell_1 = 0.17$ m
$m_3 = 0.36$ kg $\quad \ell_2 = 0.20$ m
$J_1 = 0.108$ kgm
$J_2 = 7.01 \times 10$ kgm
$J_3 = 5.00 \times 10$ kgm
$r = 4.5 \times 10^{-2}$ m
$f_1 = 6.0 \times 10$ Nms
$f_2 = 4.40 \times 10$ Nms
$f_3 = 4.40 \times 10$ Nms

$\vec{K}t = [4.88,\ 1.31,\ 5.37,\ 6.00]$
$\vec{X}(0) = [0,\ \pi/10,\ 0]$

Note that the $\vec{X}(0) = [0, \pi/10, 0.0]$ expresses the initial condition, and a disturbance $\pi/10$ (rad/s) is provided to the car part (17), where the duration of 10 ms is used as simulation interval Δt.

The pole (Si) in Part (a) in Figure 7 is expressed as:

Si = (-3±4j, -4±5j) (i = 1, 2, 3, 4)

The pole (Si) in Part (b) in Figure 7 is expressed as:

Si = (-5±4j, -6±5j)

The pole (Si) in Part (c) in Figure 7 is expressed as:

$Si = (-7\pm4j, -8\pm5j)$

The simulation results shown in Parts (a), (b), and (c) in Figure 7 indicate that the car part (17) can be returned to the balanced position ($\Theta 1 = 0$) (see a chained line shown in Figure 2) and maintained at the position thereafter. Also, with this balancing control, although the further the pole is positioned to the right half of the complex plane, the greater the control input becomes, the control system can be quickly stabilized. /620

The computer simulation results of system designs described in [2] ~ [6] all exhibit the control effectiveness of the dynamic model shown in Figure 3 and Figure 4. The coaxial two wheeler shown in Figure 2 is formed based on this theoretical argument. The schematic of the control system for the coaxial two wheeler is shown in Figure 10, and a control program shown in Part (a), (b), or (c) in Figure 11 is stored in the computer (16). The control program shown in Parts (a) and (b) in Figure 11 correspond to the linear type control system, whereas the control program shown in Part (c) in Figure 11 corresponds to the non-linear type control system.

With the linear type control program shown in Part (a) of Figure 11, the computer (16) initializes various control circuits (e.g., counter circuit, output interface circuit, data latch circuit, etc.) when a control initiation signal is inputted, and processes detection signals outputted from the rotary encoder (11) via a counter circuit. The computer then computes the

control torque (T3) using the equation (60) consisting of the sampled value Θ1 and pre-established feedback gain K, and outputs the computed control torque (T3) to the drive part via a data clutch circuit and D/A converter shown in Figure 10. The data clutch circuit holds the output data transmitted from the computer (16) until the next sampling point is reached.

With the linear type control program shown in Part (b) in Figure 11, the computer (16) initializes various control circuits (e.g., counter circuit, output interface circuit, data latch circuit, etc.) when a control initiation signal is inputted, and simultaneously processes the detection signals outputted from the rotary encoders (11, 14, 15) via a counter circuit. The computer then computes the differential values of the nth sample (Θ1, Θ2, Θ3) selected from the n groups (Θ1, Θ2, Θ3) (i) (i = 1, 2...n) [i.e., angle speeds (Θ1, Θ2, Θ3) (n)].

The computer then computes the control torque (T2 and T3) using the equation (20) comprised of sampling values (Θ1, Θ2, Θ3) (n), computed values (Θ1, Θ2, Θ3) (n), and pre-established feedback gain K. The computed control torques (T2 and T3) are output to the drive part via the data latch circuit and D/A converter shown in Figure 10.

With the non-linear type control program shown in Part (c) in Figure 11, the computer (16) performs the same process as described in the linear type control program up till the angle speed computation process using numeric value differentiation, and then computes the time-varying feedback gain $\vec{K}t$. The

computer (16) computes the control torques T2 and T3 using equations (49, 51) comprised of sampling angles ($\Theta 1$, $\Theta 2$, $\Theta 3$) (n), computed angle speed ($\Theta 1$, $\Theta 2$, $\Theta 3$) (n), and pre-set time-varying feedback gain $\vec{K}t$, and transmits those torques (T2, T3) to the drive part via the data latch circuit and D/A converter shown in Figure 8.

The following explains the numeric value differential method performed by the linear and non-linear control programs:

Sampling time Δt [i.e., between the incorporation times of ($\Theta 1$, $\Theta 2$, $\Theta 3$) (1) and ($\Theta 1$, $\Theta 2$, $\Theta 3$) (t+1)] is sufficiently small, the angle $\bar{\Theta}i$ (i = 1, 2, 3) can be approximated by a two-dimensional polynomial described below:

$$\bar{\Theta}i(t) \approx a + bt + ct^2 \qquad \ldots(52)$$

By differentiating the equation (52), the angle speed $\Theta 1(t)$ can be obtained in the following manner:

$$\bar{\Theta}i(t) = b + 2ct \qquad \ldots(53)$$

The sum of squares of the difference of observation angles $\Theta i(1)$, $\Theta i(2)$, $\Theta i(3)$, $\Theta i(4)$, and $\Theta i(5)$ at the n pieces of sampling points (5 pieces in this example)

$t1 = -\Delta t \quad t2 = -\Delta t \quad t3 = 0$

$t4 = \Delta t \quad t5 = 2\Delta t$

and $\bar{\Theta}i$ can be expressed as below:

$$\& = [\bar{\Theta}i(1) - \bar{\Theta}i(1)] + [\bar{\Theta}i(2) - \bar{\Theta}i(2)]$$
$$+ [\bar{\Theta}i(3) - \bar{\Theta}i(3)] + [\bar{\Theta}i(4) - \bar{\Theta}i(4)]$$
$$+ [\bar{\Theta}i(5) - \bar{\Theta}i(5)]$$

$$= \{\theta i(1) - (a + 2b\Delta t + 4c\Delta t^2)\}^2$$
$$+ \{\theta i(2) - (a + b\Delta t + c\Delta t^2)\}^2$$
$$+ (\theta i(3) - a)^2$$
$$+ \{\theta i(4) - (a + b\Delta t + c\Delta t^2)\}^2$$
$$+ \{\theta i(5) - (a + 2b\Delta t + 4c\Delta t^2)\}^2$$

/621

The coefficient a, b, and c of the equation (52) are determined in the following manner to minimize the value of "e":

$$a = (1/70) \cdot (-6\,\theta i(1) + 24\,\theta i(2) + 34\,\theta i(3) + 24\,\theta i(4) - 6\,\theta(5))$$

$$b = (1/10\,\Delta t) \cdot (-2\,\theta i(1) - \theta i(2) + \theta i(4) + 2\,\theta i(5))$$

$$c = (1/14\,\Delta t^2) \cdot (2\theta i(1) - \theta i(2) - 2\,\theta i(3) - \theta i(4) - 2\theta i(5))$$

By substituting the a, b, and c determined in this manner to the equation (53), the angle speed Θi(n) at each sampling point (n = 1, 2, 3, 4, 5) can be obtained. For example, the angle speed at the sampling point (t) can be expressed as below:

$$\dot{\theta} i(5) = b + 2c \cdot 2\Delta t$$
$$= (1/10\,\Delta t) \cdot (26\theta i(1) - 27\,\theta i(2) - 40\,\theta i(3) - 13\,\theta i(4) + 54\,\theta i(5))$$
$$\cdots (54)$$

That is, the angle speed Θi at the sampling point (t) is computed while the angle Θi at the sampling point is smoothed based on the past five sampling angles Θi(1) ~ Θi(5), and the computed angle speed with a smoothing effect precisely agrees

with the actual angle speed.

The length of the sampling time interval Δt affects the stability of the control system. The smaller the Δt is, the better the results become, where the computation speed of the computer (16) between two sampling points determines the interval Δt. Therefore, the equations (45) ~ (48) for computing each element of the time-varying feedback gain $\vec{Kt}$ in the non-linear type system are rewritten in the following manner:

$$k_1 = (1/b) \cdot (a E_1 - d_2 + f_1 d_1 / E_1 - c \Delta d_0 / E_1 - f_1^2 d_0 / E_1^2)$$
$$= (1/b) \cdot (a E_1 - d_2 - f_1 k_4 / \Delta - c k_3) \quad \cdots (55)$$

$$k_2 = (1/b) \cdot (a f_1 - d_3 + c \Delta d_1 / E_1 + f_1 c \Delta d_0 / E_1^2)$$
$$= (1/b) \cdot (a f_1 - d_3 - c k_4) \quad \cdots (56)$$

$$k_3 = -\Delta d_0 / E_1 \quad \cdots (57)$$

$$k_4 = (\Delta / E_1) \cdot (f_1 d_0 / E_1 - d_1)$$
$$= -(1/E_1) \cdot (d_1 \Delta + f_1 k_3) \quad \cdots (58)$$

Using equations (55) ~ (58) instead of equations (45) ~ (48), the time-varying feedback gain $\vec{Kt}$ computation time can be drastically reduced.

Parts (a), (b), and (c) in Figure 8 show the feedback control results for the coaxial two wheeler shown in Figure 4 where the wheeler was controlled using the system parameter values and initial disturbance identical to those used with the linear type control simulation performed on the dynamic model shown in Figure 5, and operated at conditional feedback gain K = [4.88, 1.31, 5.37, 6.00] obtained for each pole Si = (-3± j, -4±

2j). The curve (C11) shown in Part (a) in Figure 8 designates the variation of the slant angle Θ1 of the car part (17), and curve (C12) designates the variation of the rotational angle Θ3 of the wheel (19). The curve (C13) shown in Part (b) in Figure 8 designates the variation of the angle speed Θ1 of the car part (17), and curve (C14) designates the variation of the control torque (T3). The results shown in Parts (a) ~ (c) in Figure 8 indicate strong stability of the system during the movements of the wheels (2, 3) allowing the car part (17) to immediately regain the balanced position after experiencing a significant disturbance.

Parts (a) and (b) in Figure 9 show the feedback control results when a coaxial two wheeler shown in Figure 2 operated at the target of Θ3 = 3 rad, where the system parameters were equal to those used in the non-linear type control simulation for a dynamic model shown in Figure 3. The curve line (C15) in Part (a) /622 in Figure 9 shows the variation of the tilt angle Θ1 of the car body (17), curve line (C16) in Parts (a) and (b) in Figure 9 shows the variation of the rotational angle Θ3 of the wheel part (19), and curve line (C17) in Part (b) in Figure 9 shows the variation of the angle speed Θ1 of the car body (17). In Parts (a) and (b) in Figure 9, as the car part (17) is slightly fluctuating at the beginning, the control process for moving the wheels (2, 3) is performed in the direction preferred for stabilizing the attitude of the car body (17), controlling the wheels at short intervals. The arm part (18) also slightly

fluctuates in the same phase as that of the car body part (17) after the wheels (2, 3) start moving, and the fluctuation movements of the arm part (18) and car part (17) become synchronous approximately 7 seconds after the initiation of the wheel movement, causing the arm part (18) to greatly fluctuate. At this point, the wheels (2, 3) rapidly get close to the target position. The stability of the car part (17) during the acceleration process suppress the fluctuation of the arm part (18). The wheels (2, 4) starts decelerating at approximately 9th second. The instability of the car part (17) caused by this deceleration is compensated by the intermediate fluctuation of the arm part (18). The coaxial two wheeler stops slightly before the target position $\Theta 3 = 3$ rad. This is probably because of the friction of the solid parts of the wheel driving system.

The control effect of this device when the target position is set to $\Theta 3 = 0$ was identical to the condition after the car stopped moving [see Parts (a) and (b) in Figure 9].

When the fluctuation of the car part (17) during the motionless period of the wheeler was compared between Part (a) in Figure 8 and Part (a) in Figure 9, the attitude control method which simultaneously drives the wheel part (19) and arm part (18) could suppress the fluctuation of the car part (17) far better than the method which could only control the attitude. Therefore, the coaxial two wheeler equipped with an attitude control arm (6) shown in Figure 2 is proven to be more effective in controlling the attitude of the wheeler than the coaxial two

wheeler not equipped with an attitude control arm.

The developers of this invention conducted an attitude control experiment using only the attitude control arm (6). As a result, neither the linear or non-linear type control system could stably maintain the car body (17) at a balanced position. This is probably due to the control delay caused by the non-linear type elements (e.g., non-sensitive area of the motor (9) for driving an attitude control arm or back-lash of the gear transmission system, etc.) and the noise occurring during the angle speed computation performed based on the short-interval sampling of the slant angle of the car and attitude control arm (6) utilized with feedback control, revealing the difficult adaptation of the conventional attitude control method using only an attitude control arm (6).

This invention is not limited to the operational example described above, and any modifications [e.g., providing a steering capability to the coaxial two wheeler by connecting the wheels (2, 3) and wheel driving motor (7) via a differential movement gear system, a pair of wheels (2, 3) are independently driven to provide a steering function].

[Effectiveness of this invention]

With the first claim of this invention, the tilt angle of a car detected by the first angle detection device is sampled at short intervals, and the control torque for the wheel driving motor is computed based on the sampled data, and the feedback control is performed on the wheel driving motor based on the

computed control torque. As a result, this makes the wheels to be shifted in the slant direction of the car body to provide an immediate positional recovery of the car body.

With the second claim of this invention, the tilt angle of a car detected by the first angle detection device and wheel rotation angle detected by the secondary angle detector are sampled at short intervals; the sampled angles of the car body, rotational angle of the wheels, and angle speed computed based on those sampled angles are entered into the computer as conditional variables. Those values used as control variable and feedback gains used as coefficients are substituted in the pre-stored control equations stored in the computer to generate a control torque of the motor; the computer can control the motor by feedbacking the computed torque. As a result, when the car body is slanted, the wheels can be operated in the same slant direction of the car body to assure the car body to regain the original position.

With the third claim of this invention, the tilt angle of a car detected by the first angle detector, wheel rotation angle detected by the secondary angle detector, and slant angle of the attitude control arm detected by the third angle detector are sampled at short intervals. The pre-stored control input computation equations are computed by substituting the sampled angles of the car body, rotational angle of the wheels, slanted angle of the attitude control arm, and angle speed computed based on the sampled angles as conditional variables and feedback gains

as coefficients. The control torques for the wheel driving motor and attitude control arm driving motor are computed based on the equation computation described above, and the computer controls the wheel driving motor and attitude control arm driving motor according to the control torques, allowing the motors to be feedback-controlled. As a result, when the car body is slanted, the wheels are operated in the same direction of the slanted car body, while the control arm is rotated in the direction opposite to the slant direction, assuring the car body to regain the original attitude. With this method, the use of an attitude control arm can more assuredly maintain the balanced position of the car body than the first and second methods.

4. Simple explanation of the figures

Figure 1 shows the diagram of the device used to explain the third claim of this invention, and Figure 2 shows the cross-sectional diagram of the device shown in Figure 1. Figure 3 shows the diagram of a dynamic model of simplified system displayed in Figure 2. Figure 4 shows the diagram of the side surface of the device used in the operational example. Figure 5 shows the diagram of the side surface of a dynamic model. Parts (a) and (b) in Figure 6 show the computer simulation results of the dynamic model in Figure 5, where Part (a) shows a graph exhibiting the variation of the slant angle $\Theta 1$ and rotations angle $\Theta 3$ of the wheel (19), and Part (b) shows a graph exhibiting the variation of the angle speed Θ and rotational angle speed $\Theta 3$. Parts (a), (b), and (c) in Figure 7 shows the computer simulation

results performed on the dynamic model in Figure 3, where part (a), (b), and (c) respectively show the graph exhibiting the variation of slant angles Θ1 and Θ2 of car part 17 and arm 18 based on the selected pole Si = (-3±4j, -4±4j), pole Si = (-5±4j, 6±4j), and pole Si = (-7±4j, 8±4j). Parts (a), (b), and (c) in Figure 8 show the feedback control results of the coaxial two wheeler shown in Figure 4; where part (a) shows the graph exhibiting the variation of slant angles Θ1 and rotational angle Θ3 of wheel (19); part (b) shows the graph exhibiting the variation of rotational angle Θ3 of wheel (19); and part (c) shows the graph exhibiting the variation of control torque. Parts (a) and (b) in Figure 9 show the feedback control results of the coaxial two wheeler shown in Figure 2; where part (a) shows the graph exhibiting the variation of slant angles Θ1 and rotational angle Θ3 of wheel (19); part (b) shows the graph exhibiting the variation of rotational angles Θ3 and slant angle Θ2 of the arm part (18). Figure 10 shows the diagram of the coaxial two wheeler shown in Figures 1 and 2. Part (a) in Figure 11 shows the flow chart of a linear type control program. Part (b) in Figure 11 shows the flow chart of another linear type control program. Part (c) in Figure 11 shows the flow chart of non-linear type control program.

1... Axil; 2, 3... Wheel; 4... Car body; 6... Attitude control arm; 6a... Weight; 7... Wheel driving motor; 9... Attitude control arm driving motor; 11... First angle detection device rotary encoder; 14... Second angle detection device rotary

encoder; 15... Third angle detection device rotary encoder; 16... Computer; 17... Car body; 18... Arm; 19... Wheel part; Θ1, Θ2, Θ3... Angle; Θ1, Θ2, Θ3... Angle speed; T2, T3... Control torque; $\vec{K}$, $\vec{K}$, Kt... Feedback gain

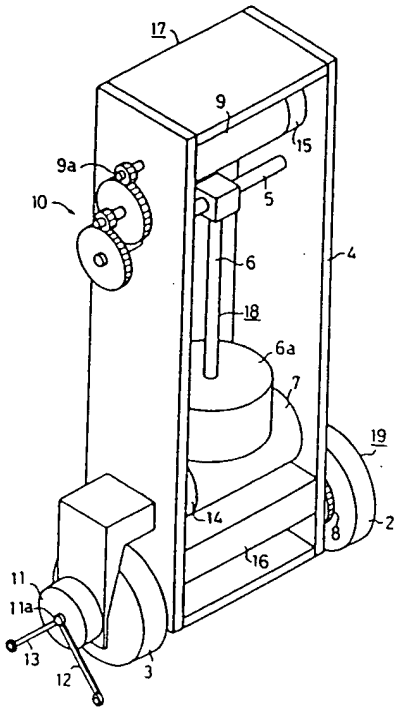

Figure 1

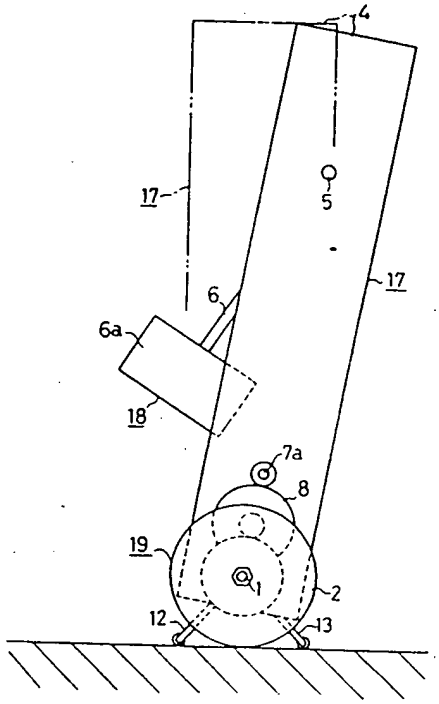

Figure 2

/624

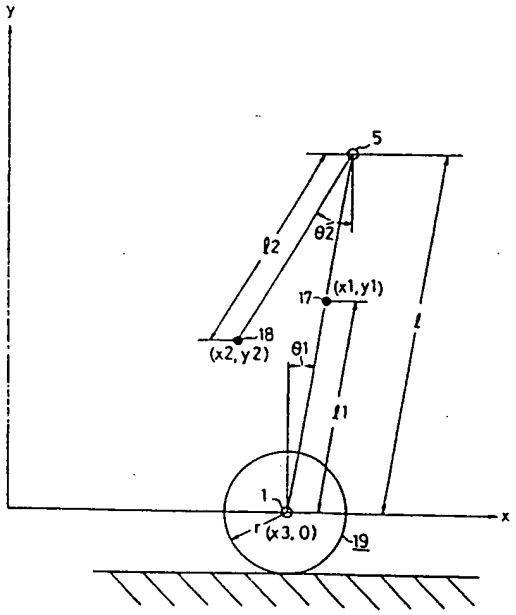

Figure 3

/625

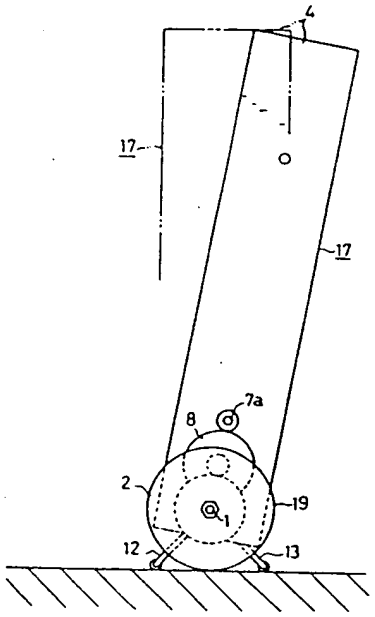

Figure 4

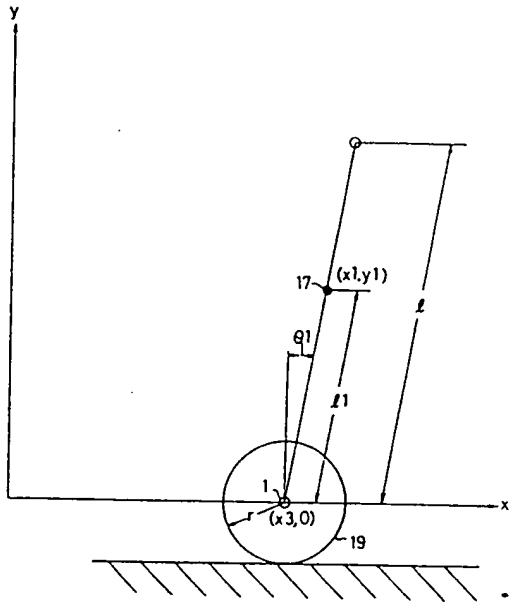

Figure 5

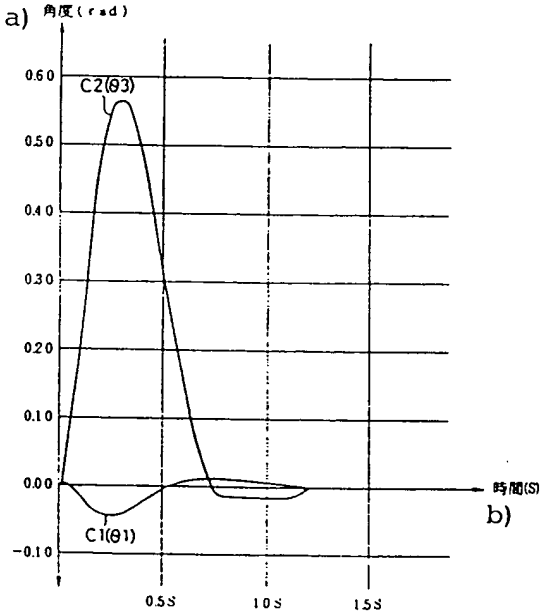

Figure 6 (a)

Key: a) Angle (rad); b) Time (S).

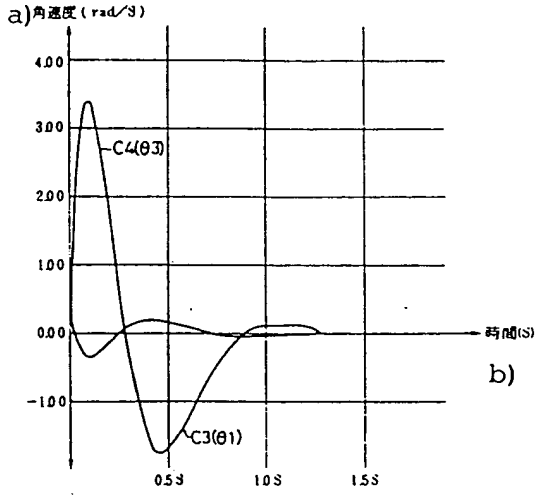

Figure 6 (b)

/626

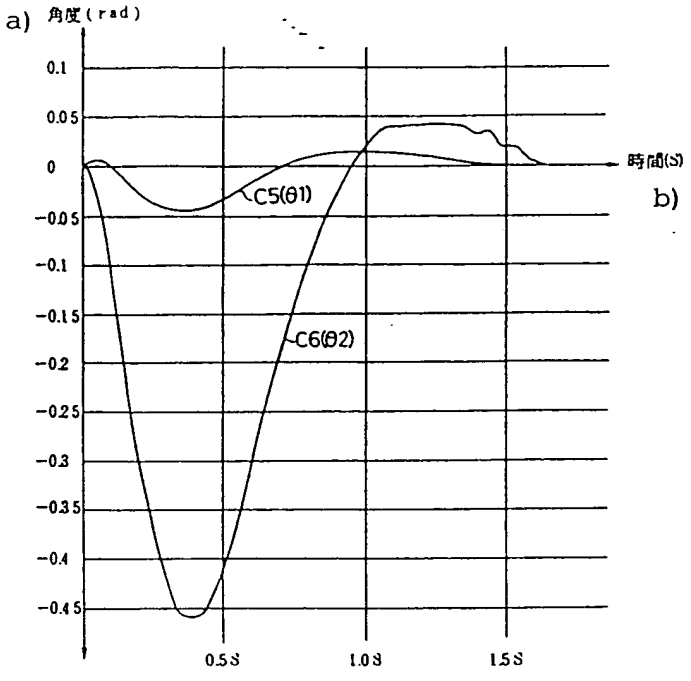

Figure 7 (a)

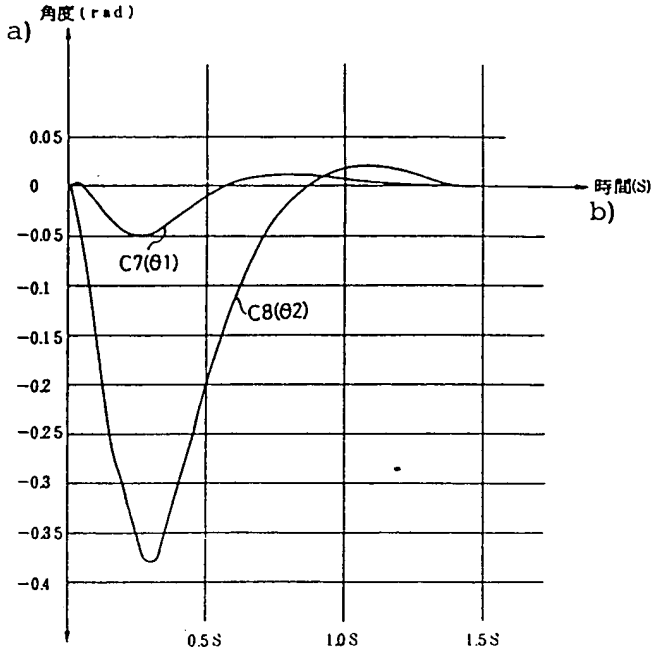

Figure 7 (b)

Key: a) Angle (rad); b) Time (S).

/627

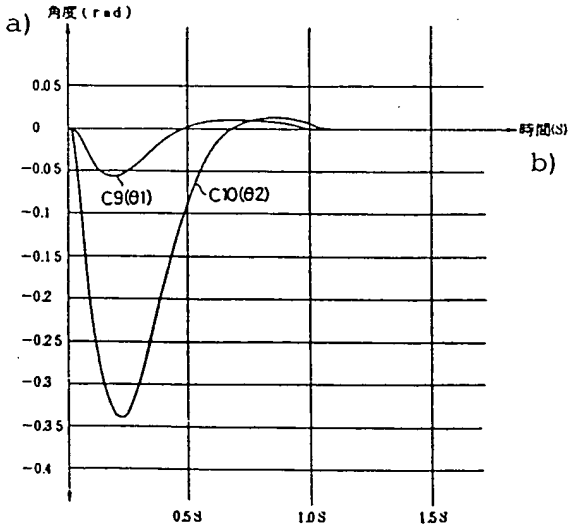

Figure 7 (c)

Key: a) Angle (rad); b) Time (S).

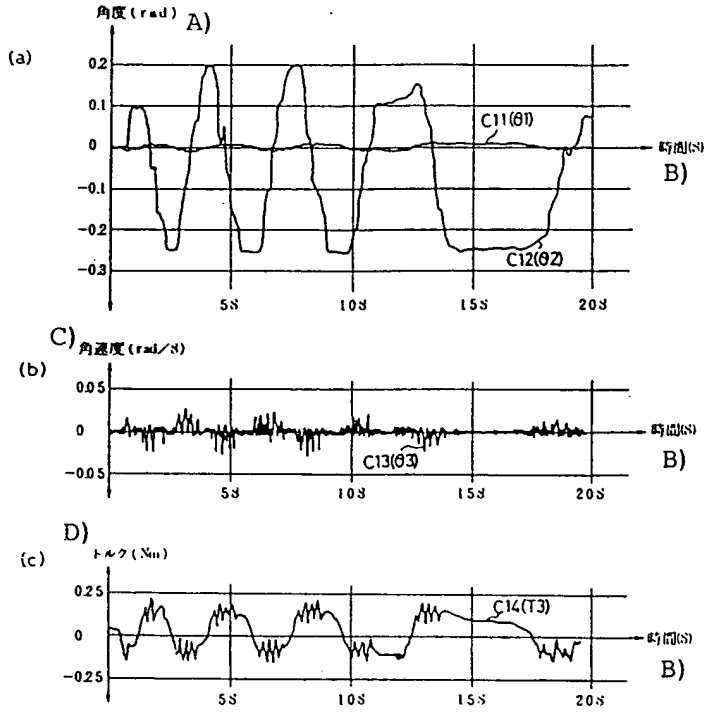

Figure 8
Key: A) Angle (rad); B) Time (S); C) Angle speed (rad/S); D) Torque (Nm).

/628

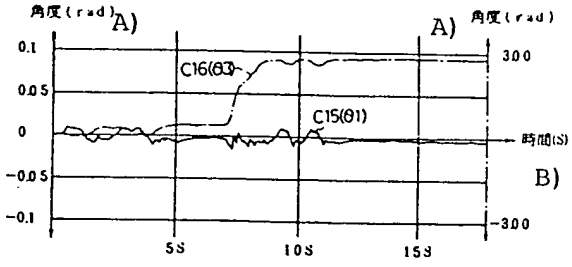

Figure 9 (a)
Key: A) Angle (rad); B) Time (S).

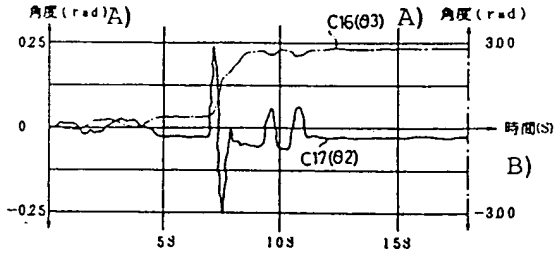

Figure 9 (b)

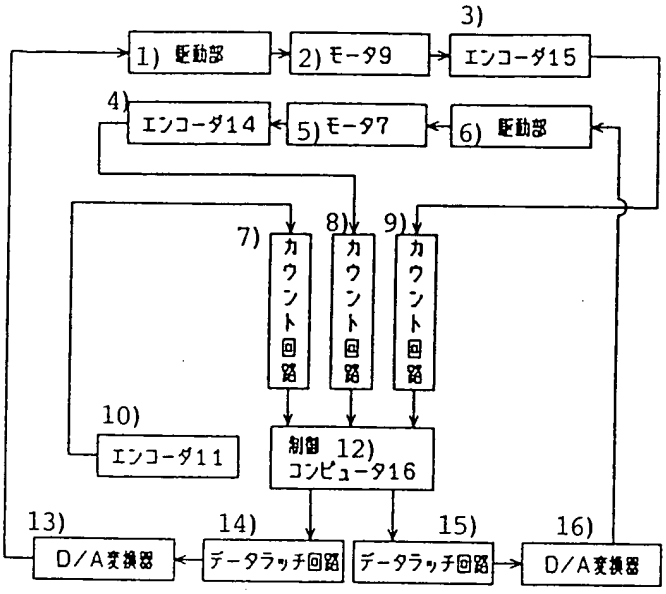

Figure 10
Key: 1) Drive part; 2) Motor 9; 3) Encoder 15; 4) Encoder 14; 5) Motor 7; 6) Drive part; 7, 8, 9) Counter circuit; 10) Encoder 11; 12) Control computer 16; 13) D/A converter; 14) Data latch circuit; 15) Data latch circuit; 16) D/A converter.

/629

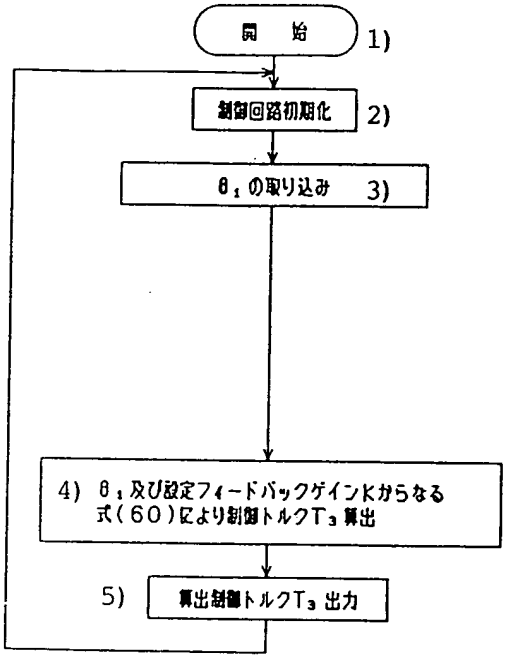

Figure 11 (a)
Key: 1) Start; 2) Control circuit initialization; 3) Θ1 incorporation; 4) Compute control torque T3 from equation (60) comprised of Θ1 and established feedback gain K; 5) Computation control torque T3 output.

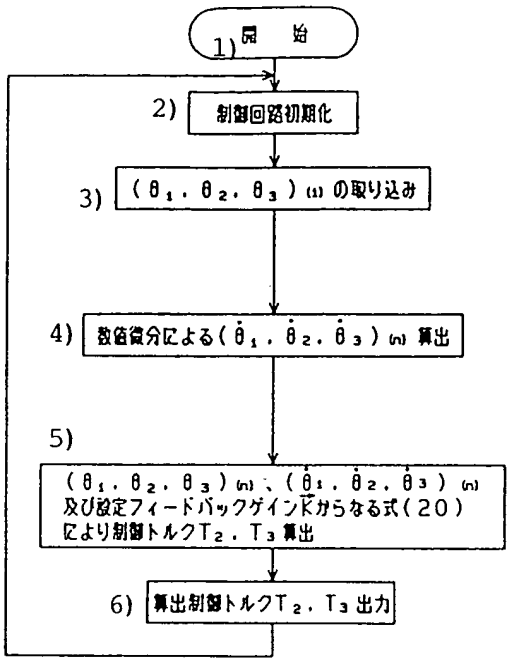

Figure 11 (b)
Key: 1) Start; 2) Control circuit initialization; 3) (Θ1, Θ2, and Θ3)(i) incorporation; 4) Compute (Θ1, Θ2, and Θ3)(n) using numeric differentiation; 5) Compute control torques T2 and T3 from equation (20) comprised of (Θ1, Θ2, and Θ3)(n) and (Θ1, Θ2, and Θ3)(n) and established feedback gain K; 6) Computation control torque T2 and T3 output

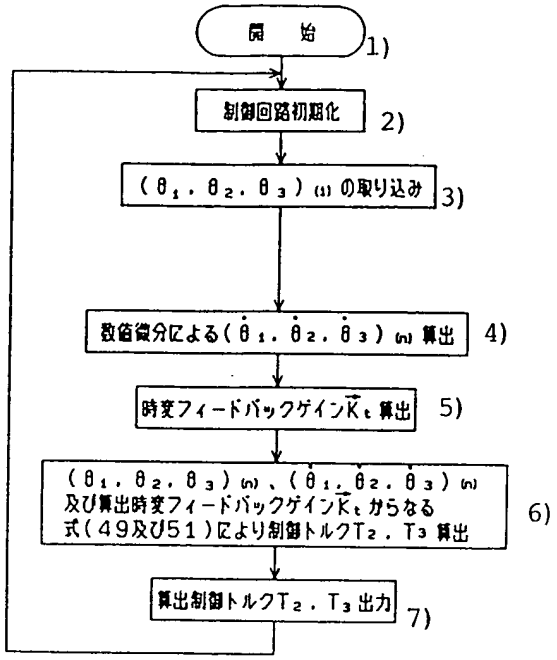

Figure 11 (c)
Key: 1) Start; 2) Control circuit initialization; 3) (Θ1, Θ2, and Θ3)(i) incorporation; 4) Compute (Θ1, Θ2, and Θ3)(n) using numeric differentiation; 5) Time-varying feedback gain Kt computation; 6) Compute control torques T2 and T3 from equation (49 and 51) comprised of (Θ1, Θ2, and Θ3)(n) and (Θ1, Θ2, and Θ3)(n) and established feedback gain K; 7) Computation control torque T2 and T3 output.